

Ultraviolet and infrared zeros of gauge theories at the four-loop order and beyond

Claudio Pica* and Francesco Sannino†

CP³-Origins, Campusvej 55, DK-5230 Odense M, Denmark

(Received 11 December 2010; published 18 February 2011)

We unveil the general features of the phase diagram for any gauge theory with fermions transforming according to distinct representations of the underlying gauge group, at the four-loop order. We classify and analyze the zeros of the perturbative beta function and discover the existence of a rich phase diagram. The anomalous dimension of the fermion masses, at the infrared stable fixed point, are presented. We show that the infrared fixed point, and associated anomalous dimension, are well described by the all-orders beta function for any theory. We also argue the possible existence, to all orders, of a nontrivial ultraviolet fixed point for gauge theories at large number of flavors.

DOI: 10.1103/PhysRevD.83.035013

PACS numbers: 12.60.Nz, 11.10.Hi, 12.38.Cy

Determining the phase structure of generic gauge theories of fundamental interactions is crucial in order to be able to select relevant extensions of the standard model of particle interactions [1]. In particular we are interested in elucidating the physics of non-Abelian gauge theories as function of the number of flavors, colors, and matter representation.

To gain a quantitative analytic understanding of the phase structure of different gauge theories we investigate the zeros of the perturbative beta function to the maximum known order and for one of the zeros also the limit of large number of flavors to all orders.

I. ZEROLOGY

We consider the perturbative expression of the beta function and the fermion mass anomalous dimension for a generic gauge theory with only fermionic matter in the $\overline{\text{MS}}$ scheme to four loops which was derived in [2,3],

$$\begin{aligned} \frac{da}{d \ln \mu^2} &= \beta(a) \\ &= -\beta_0 a^2 - \beta_1 a^3 - \beta_2 a^4 - \beta_3 a^5 + O(a^6), \quad (1) \end{aligned}$$

$$\begin{aligned} -\frac{d \ln m}{d \ln \mu^2} &= \frac{\gamma(a)}{2} \\ &= \gamma_0 a + \gamma_1 a^2 + \gamma_2 a^3 + \gamma_3 a^4 + O(a^5), \quad (2) \end{aligned}$$

where $m = m(\mu^2)$ is the renormalized (running) fermion mass and μ is the renormalization point in the $\overline{\text{MS}}$ scheme and $a = \alpha/4\pi = g^2/16\pi^2$, where $g = g(\mu^2)$ is the renormalized coupling constant of the theory.

The explicit expression of the coefficients above are reported in the Appendix for completeness. Note also that the beta function is gauge independent, order by order in perturbation theory [2]. The same also holds for the anomalous dimension of the fermion mass γ .

Here we investigate the structure of the zeros of the four-loop beta function for any matter representation and gauge group. Interestingly we find a *universal* classification of the behavior of the zeros as a function of the number of flavors n_f .

The first observation is that, due to the fact that the beta function is a polynomial of degree five in α , there are five complex zeros. Since one can factor out α^2 , the beta function will always have a double zero at the origin. The other three zeros determine the interesting properties of the theory, to this loop order. In the following we will focus on these three zeros which can be either all real or one real and two complex.

To elucidate the landscape of possible topologies we plot the real nontrivial zeros as a function of the number of flavors normalized to the one above which asymptotic freedom is lost (\bar{n}_f) in Fig. 1. Solid lines correspond to the location of the ultraviolet (UV) zeros (in black) and infrared (IR) stable fixed points (in gray/red). The shaded areas denote the regions where the beta function is positive. We have rescaled the vertical axis using the function $a^* = 2 \arctan(5a)/\pi$, mapping $[-\infty, +\infty]$ into the interval $[-1, 1]$.

The best way to read these figures is to imagine a straight vertical line corresponding to a fixed value of n_f . The intersection of this line with the solid curve determines the number of the zeros, the color of the curves, the type of zeros (if gray/red is IR and if black is UV), and finally the corresponding horizontal value is the coupling location. We term the landscape of the zeros the *zerology*.

We investigate also the negative values of α since this is the most natural mathematical setting. In fact, the properties of the pure Yang-Mills theory at negative α have already been studied on the lattice by Li and Meurice in [4]. There the authors have shown interesting relations between the positive and negative regions of α .

The beta function to the order we are considering might lead to several types of distinct topologies representing the zerology of the theory under investigation. The types and numbers of inequivalent topologies depend on the gauge group and matter representation. To our surprise, and by

*pica@cp3.sdu.dk

†sannino@cp3.sdu.dk

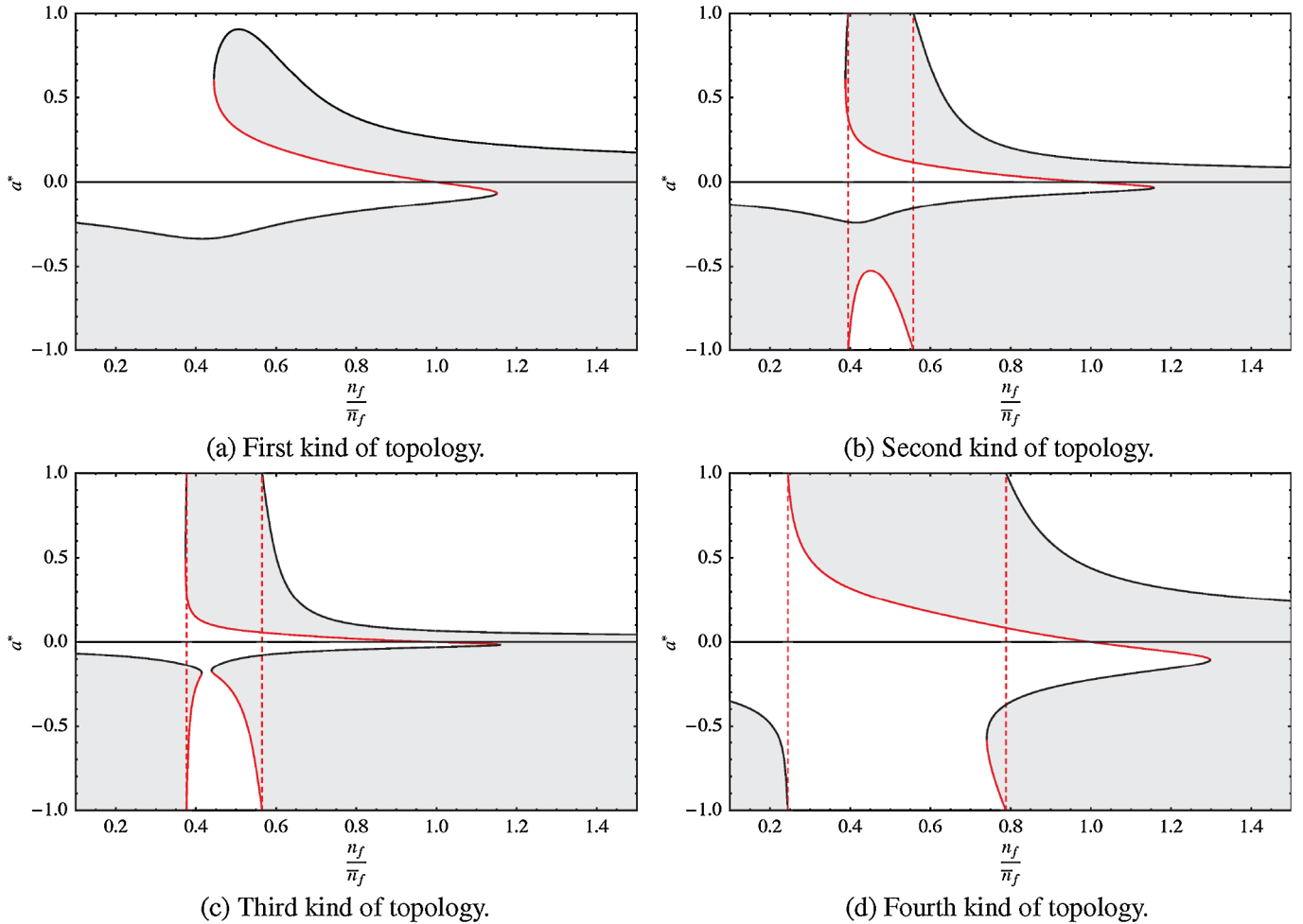


FIG. 1 (color online). The four different topologies displayed classify the entire *zerology* landscape. We show, in each plot, the regions of positive (gray) and negative (white) values of the beta function for different gauge theories. The solid lines, per each figure, are the locations of the zeros of the beta functions. The lines of UV fixed points are in black while the IR ones in gray/red. We have defined $\alpha^* = \frac{2}{\pi} \arctan(5a)$. The vertical dashed lines correspond to the location where one zero approaches infinity.

explicit enumeration, we discovered that it is possible to identify just four distinct topologies which are able to fully represent the entire *zerology* for any gauge group and matter representation. These are reported in Fig. 1.

We start by summarizing a number of general features that we have identified:

- (i) At small number of flavors there is only a negative ultraviolet zero.
- (ii) At around and above \bar{n}_f we observe the existence of three zeros, two ultraviolet and one infrared. The infrared one, near \bar{n}_f , is the Banks-Zaks [5] point. Above \bar{n}_f , the IR fixed point is now at a negative value of α and at a new critical number of flavors collides with the UV fixed point zero at a negative value of the coupling, forming a double zero. At this point the beta function is positive for any negative alpha.
- (iii) At very large number of flavors the UV fixed point, for positive values of alpha, always exists and

approaches zero asymptotically as $n_f^{-2/3}$. The explicit derivation is provided in Sec. III.

- (iv) By increasing n_f from zero there is always a critical number of flavors above which an IR fixed point emerges for positive α .

The distinguishing feature of different topologies is how the zeros merge or disappear as function of n_f .

Topology A [Fig. 1(a)] is characterized by the fact that the zeros always remain at finite values of the coupling. This means that when a zero disappears it has to annihilate with another one. This happens at two distinct locations. One at a positive value of the coupling and the other at a negative one occurring after asymptotic freedom is lost.

In topology B, represented in Fig. 1(b), as for the previous case, we still observe the merging of the IR and UV zeros at two different numbers of flavors. In this case, however, there is a region in the number of flavors, where the UV fixed point located at positive couplings reaches

TABLE I. Catalog of the four-loop zeroology for $SU(N)$, $SO(N)$, and $SP(2N)$ gauge theories with fermions transforming according to the fundamental and the two-index representations.

Representation	Topology A	Topology B	Topology C	Topology D
$SU(N)$				
Fundamental	$N = 2, 3$	$4 \leq N \leq 11$	$N \geq 12$	
Adjoint				$N \geq 2$
2-symmetric				$N \geq 2$
2-antisymmetric	$N = 3, 4, 5$	$N = 6, 7$	$8 \leq N \leq 26$	$N \geq 27$
$SO(N)$				
Fundamental		$N \leq 6$	$N = 5$	$N = 3, 4$
Adjoint				$N \geq 3$
2-symmetric				$N \geq 3$
$SP(2N)$				
Fundamental	$N = 1, 2$	$3 \leq N \leq 4$	$N \geq 5$	
Adjoint				$N \geq 1$
2-antisymmetric	$N = 3, 4$	$N = 2, 5$	$6 \leq N \leq 14$	$N \geq 15$

infinity at finite n_f and appears on the negative axis as an IR fixed point. The region where the new IR fixed point appears (on the negative coupling constant axis) ends before asymptotic freedom is lost.

The defining feature shown in Fig. 1(c) for topology C is the appearance of two more merging points at negative values of α .

In Fig. 1(d), topology D, one observes that the IR zero at a positive value of the coupling reaches infinity at a finite value of the number of flavors, which is the distinctive feature of this topology.

A new feature at the four-loop order is that two positive nontrivial zeros, one IR and the other UV, can emerge simultaneously and can annihilate at a particular value of n_f . At the two-loop level this feature does not exist and, in particular, no nontrivial ultraviolet fixed point is seen.

As an example where these topologies arise we consider $SU(N)$ with fundamental fermions as a function of N . For $N = 2$ and 3, topology A occurs. Increasing N the maximum value reached by the positive UV zero increases and for $N = 4$ it reaches infinity and therefore it enters topology B. Increasing N further the local maximum of the IR negative zero-curve increases till it pinches the UV negative zero line for $N = 11$ entering topology C. Topology D is not realized in this case. On the other hand any $SU(N)$ gauge theory with $N \geq 2$ fermions and fermions in the adjoint representation lead to topology D.

In Table I we catalog the four-loop zeroology for $SU(N)$, $SO(N)$, and $SP(2N)$ gauge theories with fermions transforming according to the fundamental and the two-index representations.

II. CONFORMAL WINDOW

The conformal window is defined as the region in theory space, as a function of number of flavors and colors, where the underlying gauge theory displays large distance conformality for a positive value of the coupling α . \bar{n}_f

constitutes the upper boundary of the conformal window and the lower boundary here is estimated by identifying for which number of flavors the theory loses the infrared fixed point at a given number of colors. Because of the fact that we are using a truncated beta function the true window will be quantitatively different.

We summarize the results for the $SU(N)$ gauge groups in Fig. 2 for the fundamental, two-index symmetric, two-index antisymmetric, and adjoint representation. The conformal window at the four-loop level is considerably wider, for any representation, when compared with the Schwinger-Dyson results [6,7] or the one obtained using the critical number of flavors where the free energy changes sign, as suggested in [8]. For completeness we

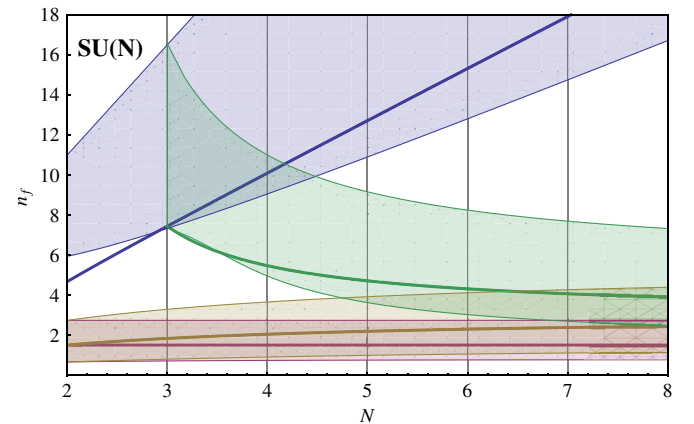


FIG. 2 (color online). Conformal window for $SU(N)$ groups for the fundamental representation (upper, light blue), two-index antisymmetric (next to the highest, light green), two-index symmetric (third window from the top, light-brown) and finally the adjoint representation (bottom, light pink). The lower boundary corresponds to the point where the infrared fixed point disappears at four loops. The solid thick lines correspond to the number of flavors for which the all-orders beta function predicts an anomalous dimension equal to unity.

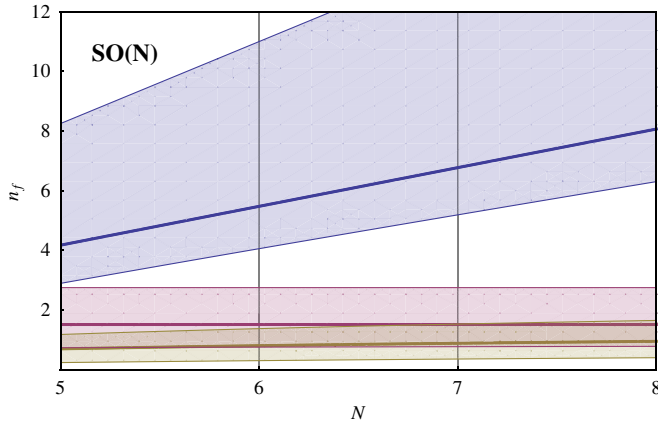


FIG. 3 (color online). Conformal window for $SO(N)$ groups for the fundamental representation (upper, light blue), two-index antisymmetric [which is the adjoint and second from the top (pink region)], and two-index symmetric (bottom window in light-brown).

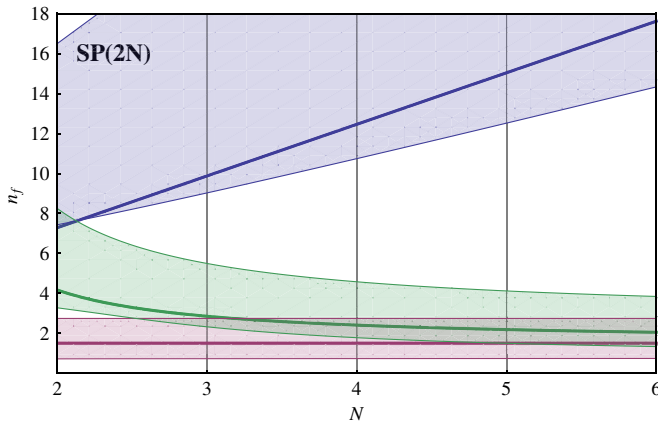


FIG. 4 (color online). Conformal window for $SP(2N)$ groups for the fundamental representation (upper, light blue), two-index antisymmetric (next to the highest, light-green), and two-index symmetric, i.e. the adjoint, (bottom window in light-pink).

also show the conformal window for the orthogonal and symplectic gauge groups, respectively, in Figs. 3 and 4. There is a universal trend toward the widening of the conformal regions with respect to earlier estimates using other nonperturbative methods.

A. All-orders beta function comparison

We have recently demonstrated the existence of a scheme in which the all-orders beta function is [9]

$$\frac{\beta(a)}{a} = -\frac{a}{3} \frac{11C_A - 2T_F n_f (2 + \Delta_F \gamma)}{1 - 2a \frac{17}{11} C_A}, \quad (3)$$

with

$$\Delta_F = 1 + \frac{7}{11} \frac{C_A}{C_F}. \quad (4)$$

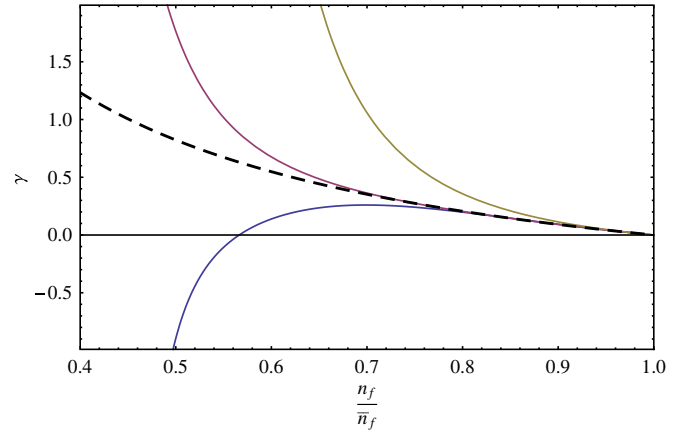


FIG. 5 (color online). Anomalous dimension of the mass, at the infrared fixed point, for $SU(3)$ as function of the number of fundamental flavors at two loops (upper brown curve), three loops (second curve from the top in magenta), all-orders (dashed curve in black), and four loops (bottom curve in blue).

This form of the beta function is similar in spirit to the one advocated in [10]. The *scheme-independent* analytical expression of the anomalous dimension of the mass at the IR positive zero is¹

$$\gamma = \frac{11C_A - 4T_F n_f}{2n_f T_F \left(1 + \frac{7}{11} \frac{C_A}{C_F}\right)}. \quad (5)$$

We plot, for reference, in Figs. 2–4 the lines corresponding to this anomalous dimension equal to unity. These are the solid thick curves for the different representations. These lines could be viewed as the lower boundary of the conformal window under the assumption that this boundary corresponds to the anomalous dimension being equal to 1. The sizes of these regions are consistent with the ones derived via gauge dualities in [12,13]. Gauge duals have also been employed in [14,15] to compute important physical correlators such as the *conformal S* parameter [16].

B. Four-loop anomalous dimensions

For illustration, we plot in Fig. 5 the anomalous dimension of the mass for the $SU(3)$ gauge theory, as a function of the number of fundamental flavors, at the IR positive zero. The three solid lines correspond, respectively, from top to bottom, to the two-, three-, and four-loop results. Perturbation theory is reliable only in a small range of flavors near \bar{n}_f . A similar behavior is observed for any other gauge group, matter representation, and different number of colors. We note that the perturbative analysis of the anomalous dimension appeared in [17], while this paper was being completed. There it has also been noted

¹The same anomalous dimension was introduced in [11] motivated by the AdS/QCD correspondence.

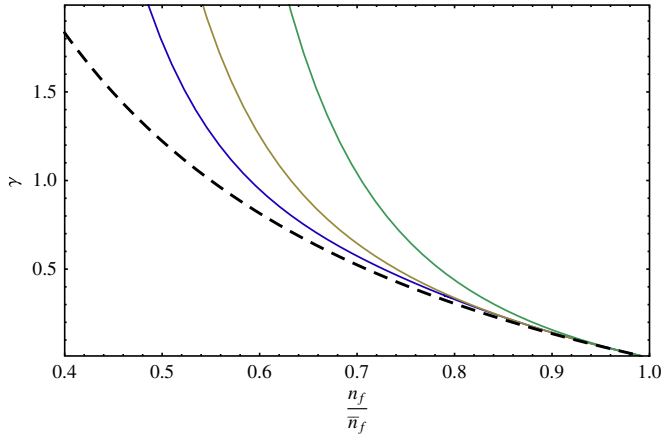


FIG. 6 (color online). Anomalous dimension of the mass, at the infrared fixed point, for $SU(2)$ as function of the number of adjoint Dirac flavors at two loops (upper green curve), three loops (second curve from the top), four loops (third curve, in blue), and all-orders (dashed curve in black).

that the anomalous dimension, to this order in perturbation theory, is smaller than for the three- and two-loop case.

Having at hand an all-order scheme-independent result, we compare it with the perturbative one. The dashed line, in Fig. 5, is the all-order anomalous dimension from (5). It is striking that the all-order result is much more well behaved than the four-loop predictions which, in this example, reach large and negative values long before losing the IR positive zero.

Because of the phenomenological interest in models of minimal walking technicolor [6,18,19] we report the anomalous dimension at the fixed point also for the $SU(2)$ gauge theory with two-adjoint fermions in Fig. 6. These theories are being subject to intensive numerical investigations via lattice simulations [20–44].

III. ASYMPTOTIC SAFETY AT LARGE n_f

To the four-loop order a positive UV zero appears for a sufficiently large number of flavors. We have already observed that the value of the zero as a function of the number of flavors decreases monotonically as $n_f^{-2/3}$ at four loops. In fact, it is possible to generalize this behavior to any finite order in perturbation theory. Consider the equation for the zeros of the beta function in which the leading powers in the number of flavors are made explicit,

$$b_0 n_f + \sum_{k=1}^{\infty} b_k n_f^k \alpha^k = 0, \quad (6)$$

where $b_0 = \beta_0/n_f$ and $b_k = \beta_k/n_f^k$. We used the fact that the first and second coefficient of the beta function are linear in the number of flavors and, in general, the successive coefficients have one extra power of n_f [45]. Therefore the coefficients b_k are finite at a large number of flavors.

We define

$$x = n_f \alpha, \quad (7)$$

and the equation at any fixed perturbative order P reads

$$b_0 n_f + \sum_{k=1}^P b_k x^k = 0. \quad (8)$$

At large n_f the solution approaches

$$x = \left(-\frac{b_0 n_f}{b_P} \right)^{1/P} \rightarrow \alpha = \left(-\frac{b_0}{b_P} \right)^{1/P} n_f^{(1-P)/P}. \quad (9)$$

There are P complex solutions for x lying on a circle in the complex plane. A positive solution exists only if b_P is positive at large n_f . This is indeed the case, at the four-loop order, for any gauge theory showing that the UV positive zero vanishes as $n_f^{-2/3}$. If this UV zero persists to higher orders its location will change although it will vanish faster as a function of n_f when increasing P , i.e. the exponent $(1-P)/P$ increases in absolute value. The case $n_f^{-2/3}$ is recovered for $P=3$.

Interestingly it is possible to sum exactly the perturbative infinite sum for the beta function, at a large number of flavors, given that the leading coefficients are known. The result is

$$\frac{3}{4n_f T_F} \frac{\beta(a)}{a^2} = 1 + \frac{H(x)}{n_f} + \mathcal{O}(n_f^{-2}). \quad (10)$$

The explicit form of $H(x)$ can be found in [45]. The important feature, here, is that $H(x)$ possesses a negative singularity at $x = 3\pi/T_F$. This demonstrates that there always is a solution for the existence of a nontrivial UV fixed point at the leading order in n_f for the following positive value of the coupling:

$$\alpha_{\text{UV}} = \frac{3\pi}{T_F n_f}. \quad (11)$$

The function $H(x)$ has also other singularities which might signal the presence of new zeros which we will not consider here, but that would be worth exploring.

Higher order terms in n_f^{-1} can, in principle, modify the result if the singularity structure is such to remove or modify its location.

A more complete discussion of the singularity structure of the coefficients of the n_f^{-1} expansion has appeared in [45] also for QED. It seems plausible that the smallest UV fixed point is an all-orders feature.

IV. CONCLUSIONS

We presented the general features of the phase diagram for any gauge theory with fermions transforming according to distinct representations of the underlying gauge group, at the four-loop order. The topology of the zeros of the

perturbative beta function has been investigated. We discovered that only four distinct topologies are sufficient to classify the gauge dynamics of any theory.

At the IR stable fixed point, for positive values of the α coupling, we computed the anomalous dimensions. We have also shown that these are well described by the all-orders beta function for any theory.

Finally, by investigating the large n_f limit we argued the possible existence, to all orders, of a nontrivial UV fixed point for any non-Abelian gauge theory at a large number of flavors.

ACKNOWLEDGMENTS

We thank the CERN Theory Institute for its kind hospitality, 25 July to 6 August 2010, where this work started

with the discovery of an all-order beta function [9] leading to anomalous dimensions in agreement with lattice estimates. We discussed the findings with several scientists since. Part of the results presented in this paper were used in [8] to compute the free-energy to the order $g^6 \ln g$. While this paper was being finalized the related paper [17] by Rytov and Shrock appeared which partially overlaps with the present work. Finally, we are happy to thank Oleg Antipin, Chris Kouvaris, Matin Mojaza, Marco Nardecchia, and Ulrik I. Søndergaard for useful discussions and careful reading of the manuscript.

APPENDIX: GROUP FACTORS AND PERTURBATIVE COEFFICIENTS

The four-loop beta function coefficients are [2]

$$\begin{aligned}
 \beta_0 &= \frac{11}{3} C_A - \frac{4}{3} T_F n_f, \\
 \beta_1 &= \frac{34}{3} C_A^2 - 4 C_F T_F n_f - \frac{20}{3} C_A T_F n_f, \\
 \beta_2 &= \frac{2857}{54} C_A^3 + 2 C_F^2 T_F n_f - \frac{205}{9} C_F C_A T_F n_f - \frac{1415}{27} C_A^2 T_F n_f + \frac{44}{9} C_F T_F^2 n_f^2 + \frac{158}{27} C_A T_F^2 n_f^2, \\
 \beta_3 &= C_A^4 \left(\frac{150653}{486} - \frac{44}{9} \zeta_3 \right) + C_A^3 T_F n_f \left(-\frac{39143}{81} + \frac{136}{3} \zeta_3 \right) + C_A^2 C_F T_F n_f \left(\frac{7073}{243} - \frac{656}{9} \zeta_3 \right) \\
 &\quad + C_A C_F^2 T_F n_f \left(-\frac{4204}{27} + \frac{352}{9} \zeta_3 \right) + 46 C_F^3 T_F n_f + C_A^2 T_F^2 n_f^2 \left(\frac{7930}{81} + \frac{224}{9} \zeta_3 \right) + C_F^2 T_F^2 n_f^2 \left(\frac{1352}{27} - \frac{704}{9} \zeta_3 \right) \\
 &\quad + C_A C_F T_F^2 n_f^2 \left(\frac{17152}{243} + \frac{448}{9} \zeta_3 \right) + \frac{424}{243} C_A T_F^3 n_f^3 + \frac{1232}{243} C_F T_F^3 n_f^3 + \frac{d_A^{abcd} d_A^{abcd}}{N_A} \left(-\frac{80}{9} + \frac{704}{3} \zeta_3 \right) \\
 &\quad + n_f \frac{d_F^{abcd} d_A^{abcd}}{N_A} \left(\frac{512}{9} - \frac{1664}{3} \zeta_3 \right) + n_f^2 \frac{d_F^{abcd} d_F^{abcd}}{N_A} \left(-\frac{704}{9} + \frac{512}{3} \zeta_3 \right). \tag{A1}
 \end{aligned}$$

TABLE II. Relevant group factors for $SU(N)$, $SO(N)$ and $SP(2N)$.

Representation	N_F	T_F	C_F	$d_F^{abcd} d_A^{abcd} / N_F$	$d_F^{abcd} d_F^{abcd} / N_F$
<i>SU(N)</i>					
Fundamental	N	$\frac{1}{2}$	$\frac{N^2-1}{2N}$	$\frac{1}{48} (N-1)(N+1)(N^2+6)$	$\frac{(N-1)(N+1)(N^4-6N^2+18)}{96N^3}$
Adjoint	N^2-1	N	N	$\frac{1}{24} N^2(N+36)$	$\frac{1}{4} N^2(N^2+36)$
2-symmetric	$\frac{1}{2} N(N+1)$	$\frac{N+2}{2}$	$N - \frac{2}{N} + 1$	$\frac{1}{24} (N-1)(N+2)(N^2+6N+24)$	$\frac{(N-1)(N+2)(N^5-14N^4+72N^3-48N^2-288N+576)}{48N^3}$
2-antisymmetric	$\frac{1}{2} (N-1)N$	$\frac{N-2}{2}$	$N - \frac{2}{N} - 1$	$\frac{1}{24} (N-2)(N+1)(N^2-6N+24)$	$\frac{(N-2)(N+1)(N^5+14N^4+72N^3+48N^2-288N-576)}{48N^3}$
<i>SO(N)</i>					
Fundamental	N	1	$\frac{N-1}{2}$	$\frac{(N-1)(N^5-10N^4+315N^3-1250N^2+1840N-1408)}{384(N^2-N+4)}$	$\frac{(N-1)(N^4-2N^3+107N^2-106N+128)}{384(N^2-N+4)}$
Adjoint	$\frac{1}{2} (N-1)N$	$N-2$	$N-2$	$\frac{N^6-185N^5+875N^4-6170N^3+17600N^2-25728N+18944}{192(N^2-N+4)}$	$\frac{N^6-18N^5+875N^4-6170N^3+17600N^2-25728N+18944}{192(N^2-N+4)}$
2-symmetric	$\frac{1}{2} (N^2+N-2)$	$N+2$	N	$\frac{N(N^5-4N^4+723N^3-2576N^2+2752N-1792)}{192(N^2-N+4)}$	$\frac{N(N^5+12N^4+787N^3+1824N^2+1344N+3328)}{192(N^2-N+4)}$
<i>SP(2N)</i>					
Fundamental	$2N$	$\frac{1}{2}$	$\frac{1}{2} (2N+1)$	$\frac{(2N+1)(4N^5+20N^4+15N^3-50N^2+10N+101)}{96(2N^2+N+2)}$	$\frac{(2N+1)(8N^4+8N^3-26N^2-14N+49)}{384(2N^2+N+2)}$
Adjoint	$N(2N+1)$	$N+1$	$N+1$	$\frac{4N^6+36N^5+125N^4+85N^3-100N^2+216N+434}{24(2N^2+N+2)}$	$\frac{4N^6+36N^5+125N^4+85N^3-100N^2+216N+434}{24(2N^2+N+2)}$
2-antisymmetric	$N(2N-1)-1$	$N-1$	N	$\frac{N(4N^5+8N^4-27N^3-62N^2+238N+374)}{24(2N^2+N+2)}$	$\frac{N(4N^5-24N^4+37N^3+138N^2+6N-386)}{24(2N^2+N+2)}$

Here ζ_x is the Riemann zeta function evaluated at x , T_F^a with $a = 1, \dots, N_F$ are the generators for a generic representation F with dimension N_F . The generators are normalized via $\text{tr}(T_F^a T_F^b) = T_F \delta^{ab}$ and the quadratic Casimirs are $[T_F^a T_F^a]_{ij} = C_F \delta_{ij}$. The subscript A refers to the adjoint representation in the formulas in the text. Here the number of fermions is indicated by n_f .

The symbols d_F^{abcd} are the fourth-order group invariants expressed in terms of contractions between the following fully symmetrical tensors:

$$d_F^{abcd} = \frac{1}{6} \text{Tr}[T_F^a T_F^b T_F^c T_F^d + T_F^a T_F^b T_F^d T_F^c + T_F^a T_F^c T_F^b T_F^d + T_F^a T_F^c T_F^d T_F^b + T_F^a T_F^d T_F^b T_F^c + T_F^a T_F^d T_F^c T_F^b]. \quad (\text{A2})$$

For readers' convenience we provide in Table II the relevant group factors.

The coefficients of the anomalous dimension to four-loops are [3]

$$\begin{aligned} \gamma_0 &= 3C_F \\ \gamma_1 &= \frac{3}{2}C_F^2 + \frac{97}{6}C_F C_A - \frac{10}{3}C_F T_F n_f \\ \gamma_2 &= \frac{129}{2}C_F^3 - \frac{129}{4}C_F^2 C_A + \frac{11413}{108}C_F C_A^2 + C_F^2 T_F n_f (-46 + 48\zeta_3) + C_F C_A T_F n_f \left(-\frac{556}{27} - 48\zeta_3\right) - \frac{140}{27}C_F T_F^2 n_f^2 \\ \gamma_3 &= C_F^4 \left(-\frac{1261}{8} - 336\zeta_3\right) + C_F^3 C_A \left(\frac{15349}{12} + 316\zeta_3\right) + C_F^2 C_A^2 \left(-\frac{34045}{36} - 152\zeta_3 + 440\zeta_5\right) \\ &\quad + C_F C_A^3 \left(\frac{70055}{72} + \frac{1418}{9}\zeta_3 - 440\zeta_5\right) + C_F^3 T_F n_f \left(-\frac{280}{3} + 552\zeta_3 - 480\zeta_5\right) + C_F^2 C_A T_F n_f \left(-\frac{8819}{27} + 368\zeta_3\right) \\ &\quad - 264\zeta_4 + 80\zeta_5) + C_F C_A^2 T_F n_f \left(-\frac{65459}{162} - \frac{2684}{3}\zeta_3 + 264\zeta_4 + 400\zeta_5\right) + C_F^2 T_F^2 n_f^2 \left(\frac{304}{27} - 160\zeta_3 + 96\zeta_4\right) \\ &\quad + C_F C_A T_F^2 n_f^2 \left(\frac{1342}{81} + 160\zeta_3 - 96\zeta_4\right) + C_F T_F^3 n_f^3 \left(-\frac{664}{81} + \frac{128}{9}\zeta_3\right) + \frac{d_F^{abcd} d_A^{abcd}}{N_F} (-32 + 240\zeta_3) \\ &\quad + n_f \frac{d_F^{abcd} d_F^{abcd}}{N_F} (64 - 480\zeta_3). \end{aligned} \quad (\text{A3})$$

The results of (A1) and (A3) are valid for an arbitrary semisimple compact Lie group. The result for QED [i.e. the group $U(1)$] is included in Eq. (A3) by substituting $C_A = 0$, $d_A^{abcd} = 0$, $C_F = 1$, $T_F = 1$, $(d_F^{abcd})^2 = 1$, $N_F = 1$.

These coefficients were obtained in an arbitrary covariant gauge for the gluon field and are gauge independent.

-
- | | |
|---|--|
| <p>[1] F. Sannino, <i>Acta Phys. Pol. B</i> 40, 3533 (2009).
 [2] T. van Ritbergen, J. A. M. Vermaseren, and S. A. Larin, <i>Phys. Lett. B</i> 400, 379 (1997).
 [3] J. A. M. Vermaseren, S. A. Larin, and T. van Ritbergen, <i>Phys. Lett. B</i> 405, 327 (1997).
 [4] L. Li and Y. Meurice, <i>Phys. Rev. D</i> 71, 016008 (2005).
 [5] T. Banks and A. Zaks, <i>Nucl. Phys.</i> B196, 189 (1982).
 [6] F. Sannino and K. Tuominen, <i>Phys. Rev. D</i> 71, 051901 (2005).
 [7] D. D. Dietrich and F. Sannino, <i>Phys. Rev. D</i> 75, 085018 (2007).
 [8] M. Mojaza, C. Pica, and F. Sannino, <i>Phys. Rev. D</i> 82, 116009 (2010).
 [9] C. Pica and F. Sannino, arXiv:1011.3832.
 [10] T. A. Ryttov and F. Sannino, <i>Phys. Rev. D</i> 78, 065001 (2008).
 [11] O. Antipin and K. Tuominen, arXiv:0912.0674.
 [12] F. Sannino, <i>Phys. Rev. D</i> 80, 065011 (2009).</p> | <p>[13] F. Sannino, <i>Nucl. Phys.</i> B830, 179 (2010).
 [14] F. Sannino, <i>Phys. Rev. Lett.</i> 105, 232002 (2010).
 [15] S. Di Chiara, C. Pica, and F. Sannino, arXiv:1008.1267.
 [16] F. Sannino, <i>Phys. Rev. D</i> 82, 081701 (2010).
 [17] T. A. Ryttov and R. Shrock, arXiv:1011.4542.
 [18] D. K. Hong, S. D. H. Hsu, and F. Sannino, <i>Phys. Lett. B</i> 597, 89 (2004).
 [19] D. D. Dietrich, F. Sannino, and K. Tuominen, <i>Phys. Rev. D</i> 72, 055001 (2005).
 [20] S. Catterall and F. Sannino, <i>Phys. Rev. D</i> 76, 034504 (2007).
 [21] L. Del Debbio, M. T. Frandsen, H. Panagopoulos, and F. Sannino, <i>J. High Energy Phys.</i> 06 (2008) 007.
 [22] Y. Shamir, B. Svetitsky, and T. DeGrand, <i>Phys. Rev. D</i> 78, 031502 (2008).
 [23] A. Deuzeman, M. P. Lombardo, and E. Pallante, <i>Phys. Lett. B</i> 670, 41 (2008).
 [24] L. Del Debbio, A. Patella, and C. Pica, <i>Phys. Rev. D</i> 81, 094503 (2010).</p> |
|---|--|

- [25] S. Catterall, J. Giedt, F. Sannino, and J. Schneible, *J. High Energy Phys.* **11** (2008) 009.
- [26] L. Del Debbio, A. Patella, and C. Pica, Proc. Sci., LATTICE2008 (2008) 064 [[arXiv:0812.0570](#)].
- [27] T. DeGrand, Y. Shamir, and B. Svetitsky, *Phys. Rev. D* **79**, 034501 (2009).
- [28] A. J. Hietanen, J. Rantaharju, K. Rummukainen, and K. Tuominen, *J. High Energy Phys.* **05** (2009) 025.
- [29] T. Appelquist, G. T. Fleming, and E. T. Neil, *Phys. Rev. D* **79**, 076010 (2009).
- [30] A. J. Hietanen, K. Rummukainen, and K. Tuominen, *Phys. Rev. D* **80**, 094504 (2009).
- [31] A. Deuzeman, M. P. Lombardo, and E. Pallante, *Phys. Rev. D* **82**, 074503 (2010).
- [32] A. Hasenfratz, *Phys. Rev. D* **80**, 034505 (2009).
- [33] L. Del Debbio, B. Lucini, A. Patella, C. Pica, and A. Rago, *Phys. Rev. D* **80**, 074507 (2009).
- [34] Z. Fodor, K. Holland, J. Kuti, D. Nogradi, and C. Schroeder, *Phys. Lett. B* **681**, 353 (2009).
- [35] Z. Fodor, K. Holland, J. Kuti, D. Nogradi, and C. Schroeder, *J. High Energy Phys.* **11** (2009) 103.
- [36] T. DeGrand, *Phys. Rev. D* **80**, 114507 (2009).
- [37] S. Catterall, J. Giedt, F. Sannino, and J. Schneible, [arXiv:0910.4387](#).
- [38] F. Bursa, L. Del Debbio, L. Keegan, C. Pica, and T. Pickup, *Phys. Rev. D* **81**, 014505 (2010).
- [39] E. Bilgici *et al.*, *Phys. Rev. D* **80**, 034507 (2009).
- [40] J. B. Kogut and D. K. Sinclair, *Phys. Rev. D* **81**, 114507 (2010).
- [41] A. Hasenfratz, *Phys. Rev. D* **82**, 014506 (2010).
- [42] L. Del Debbio, B. Lucini, A. Patella, C. Pica, and A. Rago, *Phys. Rev. D* **82**, 014509 (2010).
- [43] L. Del Debbio, B. Lucini, A. Patella, C. Pica, and A. Rago, *Phys. Rev. D* **82**, 014510 (2010).
- [44] S. Catterall, L. Del Debbio, J. Giedt, and L. Keegan, Proc. Sci. LATTICE2010 (2010) 057 [[arXiv:1010.5909](#)].
- [45] For a large n_f review, see B. Holdom, *Phys. Lett. B* **694**, 74 (2010).